Theoretical study of Fe(CO)n -

ARTICLE *in* THE JOURNAL OF PHYSICAL CHEMISTRY · APRIL 1995

Impact Factor: 2.78 · DOI: 10.1021/j100016a029

2 AUTHORS, INCLUDING:

C. W. Bauschlicher
NASA
759 PUBLICATIONS **23,479** CITATIONS

SEE PROFILE

Reprinted from The Journal of Physical Chemistry, 1995, 99.

Theoretical Study of $Fe(CO)_n^-$

Alessandra Ricca and Charles W. Bauschlicher, Jr.*

NASA Ames Research Center, Moffett Field, California 94035

Received: October 19, 1994; In Final Form: February 2, 1995[⊗]

The structures and CO binding energies are computed for $Fe(CO)_n^-$ using a hybrid density functional theory (DFT) approach. The structures and ground states can be explained in terms of maximizing the Fe to CO $2\pi^*$ donation and minimizing Fe−CO 5σ repulsion. The trends in the CO binding energies for $Fe(CO)_n^-$ and the differences between the trends for $Fe(CO)_n^-$ and $Fe(CO)_n$ are also explained. For $Fe(CO)_n^-$, the second, third, and fourth CO bonding energies are in good agreement with experiment, while the first is too small. The first CO binding is also too small using the coupled cluster singles and doubles approach including a perturbational estimate of the connected triple excitations.

I. Introduction

The successive ligand binding energies offer insight into how the bonding in metal−ligand systems is changing with the number of ligands. For example, a large change in the binding energies could indicate a change in the bonding mechanism. For $Cu(H_2O)_n^+$ there is a large decrease for the third water binding energy. Calculations have shown[1] that $sd\sigma$ hybridization, which is very important in reducing the metal−ligand repulsion for the first two waters, is lost with the addition of the third ligand and is therefore responsible for the large decrease in the third binding energy. For $Fe(CO)_n^+$ there is a similar drop[2] in binding energy for the third CO. Because $Fe(CO)_2^+$ is a quartet state and $Fe(CO)_5^+$ is a doublet state, it is difficult to identify the origin of the decrease in the third ligand binding energy for $Fe(CO)_n^+$; it could be from the loss of $sd\sigma$ hybridization as in $Cu(H_2O)_n^+$ or it could be due to a change in the Fe spin state. Calculations have shown[2] that the decrease in the third CO binding energy in $Fe(CO)_n^+$ is due to loss of $sd\sigma$ hybridization and that the decrease in the fifth CO binding energy is due to the change in the Fe spin.

These examples show the importance of performing accurate calculations to aid in the understanding of the changes in bonding that occur as the number of ligands is changed. Conversely it is important to have accurate experimental binding energies to compare with the calculations. Agreement between theory and experiment shows that theory is correctly describing the bonding.

The successive CO bond energies of $Fe(CO)_4^-$ have been determined experimentally by Sunderlin, Wang, and Squires.[3] The CO binding energies increase for the first three CO molecules and then decrease slightly for the fourth CO. This trend is very different from that observed for positive ions containing Fe, such as $Fe(CO)_n^+$,[4-6] $Fe(H_2O)_n^+$,[7] and $Fe(CH_4)_n^+$,[8] where there is a large decrease in the third ligand binding energy. The trend for $Fe(CO)_n^-$ is also different from that for the neutral $Fe(CO)_n$, where there is a dramatic increase in the second CO binding energy followed by a decrease for the third.[3] However for both $Fe(CO)_n^-$ and $Fe(CO)_n$ the third binding energy is similar to the fourth. In this work we consider the $Fe(CO)_n^-$ systems with $n = 1-4$. Our goals are to understand the nature of the bonding and to explain the trends in the experimental CO binding energies.

In addition to the binding energies for all four CO molecules, there is detailed information about $FeCO^-$. Villalta and Leopold[9] have obtained the negative ion photoelectron spectra of $FeCO^-$ at an instrumental resolution considerably improved over that employed by Engelking and Lineberger.[10] They have assigned the ground state of $FeCO^-$ as a $^4\Sigma^-$ state with an Fe^- occupation of $3d\delta^2 3d\pi^4 sd\sigma^2 sp\sigma^1$ and they have suggested that the bonding is derived from the ^4F state of Fe^-. They measured the Fe−C stretching frequency (465 ± 10 cm^{-1}) and the bending frequency (230 ± 40 cm^{-1}) of $FeCO^-$. The high Fe−C stretching frequency is consistent with a strong (33.7 ± 3.5 kcal/mol [3]) Fe−CO bond.

Castro, Salahub, and Fournier[11] have studied $FeCO^-$ using a linear combination of Gaussian-type orbital-density functional (LCGTO-DF) method. Their results confirm the assignment by Villalta and Leopold of a $^4\Sigma^-$ ground state. Castro *et al.* obtain an Fe−C stretching harmonic frequency (566 cm^{-1}) higher than the experimental fundamental and a bending frequency (272 cm^{-1}) close to that from experiment. Their CO binding energy was in good agreement with experiment. However, it should be noted that when they applied[11] the same method to $FeCO^+$, they obtained a binding energy that was significantly too large.

II. Methods

The Fe basis set is a [8s 4p 3d] contraction of the (14s 9p 5d) primitive set developed by Wachters.[12] The s and p spaces are contracted using contraction number 3, while the d space is contracted (311). To this basis set two diffuse p functions are added; these are the functions optimized by Wachters multiplied by 1.5. A diffuse d function[13] and an f polarization function ($\alpha = 1.339$) are added. To describe the negative ion, a diffuse s and p function ($\alpha(s) = 0.013963$ and $\alpha(p) = 0.02092$) are added. The C and O basis sets are [4s 3p] contractions of the (9s 5p) primitive set optimized by Huzinaga.[14] The s space is contracted (5211). A d polarization function is added; the exponents are 0.75 for carbon and 0.85 for oxygen. Only the pure spherical harmonic components of the basis functions are used in all calculations. We perform one calibration calculation using a large basis set. The C and O basis sets are the augmented-correlation-consistent polarized valence quadruple zeta basis sets,[15] without the diffuse g function. The Fe basis set is the (20s 15p 10d 6f 4g)/[(6 + 1)s (5 + 1)p 4d 3f 2g] atomic natural orbital basis set[16] with a diffuse s (0.012) and p (0.009) function added.

In the density functional theory (DFT) calculations we use a modification[17] of the original Becke hybrid functional[18] of the

[⊗] Abstract published in *Advance ACS Abstracts*, April 1, 1995.

0022-3654/95/2099-5922$09.00/0

TABLE 1: Summary of Successive Binding Energies, in kcal/mol [c]

		present work		
	expt[a]	B3LYP	CCSD(T)[b]	$2\pi^*$ pop
$Fe^- - CO$	33.1 ± 3.5	19.7	23.1 (24.7)	0.55
$FeCO^- - CO$	34.9 ± 3.5	34.4		0.59
$Fe(CO)_2^- - CO$	41.5 ± 3.5	45.3		0.82
$Fe(CO)_3^- - CO$	40.9 ± 2.5	38.8		0.74

[a] Sunderlin, Wang, and Squires.[3] The values have been converted to 0 K using the computed results. [b] The B3LYP frequencies are used to compute the zero-point energies. The value in parentheses is computed using the large basis set. [c] The dissociation energy for $Fe^- - CO$ is computed to Fe^- $^4F(3d^74s^2)$. The per CO $2\pi^*$ population is also given.

form

$$(1 - A)E_x^{\text{Slater}} + AE_x^{\text{HF}} + BE_x^{\text{Becke}} + CE_c^{\text{LYP}} + (1 - C)E_c^{\text{VWN}}$$

where E_x^{Slater} is the Slater exchange, E_x^{HF} is the Hartree−Fock exchange, E_x^{Becke} is the gradient part of the exchange functional of Becke,[19] E_c^{LYP} is the correlation functional of Lee, Yang, and Parr,[20] E_c^{VWN} is the correlation functional of Vosko, Wilk, and Nusair,[21] and A, B, and C are the coefficients determined by Becke[18] using his three-parameter fit to the experimental heats of formation for his original hybrid functional. The modified functional is denoted B3LYP and is used to optimize the geometries and to compute the frequencies. The computed vibrational frequencies confirm that the structures correspond to minima.

We also optimize the geometry and compute the binding energy of $FeCO^-$ using the coupled-cluster singles and doubles approach[22] including a perturbational estimate of the triples excitations[23] [denoted CCSD(T)]. The CCSD(T) approach is based on a spin-unrestricted self-consistent-field wave function. Only the valence electrons are correlated. In addition, we compute the $FeCO^-$ binding energy using the CCSD(T) approach using the large basis set at the B3LYP geometry. These large basis set CCSD(T) calculations use the restricted open-shell CCSD(T) approach.[24]

All calculations were performed using Gaussian 92/DFT,[25] except for the large basis set CCSD(T) calculations which were performed using MOLPRO 94.[26] The visualization system MOLEKEL[27] has been used to represent the molecular orbitals. The calculations were performed using the NASA Ames Central Computer Facility CRAY C90 or Computational Chemistry IBM RISC System/6000 computers.

III. Results and Discussion

For $FeCO^-$, $Fe(CO)_2^-$, and $Fe(CO)_3^-$ we consider both doublet and quartet states. For $FeCO^-$ the quartet state is significantly lower than the doublet state. For $Fe(CO)_2^-$ the quartet and the doublet states are close in energy with the doublet state 2.5 kcal/mol below the quartet state. This energy difference is too small to definitively determine the ground state of $Fe(CO)_2^-$. To compute the binding energies, we use the doublet state as it is lower in energy. For $Fe(CO)_3^-$ the doublet state is considerably lower than the quartet state. Because low-spin states are stabilized by additional ligands, $Fe(CO)_4^-$ must have a doublet ground state, and therefore, we study only this state.

The computed binding energies, geometries, and harmonic frequencies are reported in Tables 1−3. We first discuss the nature of the bonding. The ground state of $FeCO^-$ is $^4\Sigma^-$ with an Fe^- occupation of $3d\delta^23d\pi^4sd\sigma^2sp\sigma^1$. This state is derived from a $3d^74s^2$ Fe^- configuration, but a 3d population of 6.61 indicates that a mixing of $3d^6$ character also occurs as a result of the large Fe to CO $2\pi^*$ donation. The $3d\pi^4$ occupancy maximizes this 3d to CO $2\pi^*$ donation. This donation results in a C−O bond length considerably longer than that in free CO and longer than that in FeCO and a C−O harmonic frequency that is 347 cm^{-1} smaller than that in free CO and 167 cm^{-1} smaller than that in FeCO at the same level of theory.[28] Thus, the addition of an electron to Fe increases the 3d to CO $2\pi^*$ donation relative to FeCO, as expected. The (Fe 4s)−(CO 5σ) interaction is repulsive in character, but the repulsion is reduced by both $sd\sigma$ and sp hybridization. The extra σ electron in $FeCO^-$ relative to FeCO results in an Fe−C distance that is larger for $FeCO^-$ than for FeCO.

The $^2\Pi_u$ and $^4\Pi_u$ states of $Fe(CO)_2^-$ have $D_{\infty h}$ symmetry and have an Fe $3d^74s^1$ occupation. That is, the bonding is $Fe^0(CO)_2^-$ in character, where the electron on the $(CO)_2$ subunit is in the $2\pi^*$ orbital. The Fe occupation is $3d\delta^23d\pi^4sd\sigma^2$ in both states, with the $2\pi^*$ electron high-spin-coupled to the open-shell 3d electrons in the quartet state and low-spin-coupled in the doublet state. This bonding mechanism is somewhat different from that in $FeCO^-$. In $FeCO^-$ there are three Fe σ valence electrons

TABLE 2: Computed Geometrical Parameters Using B3LYP[c]

	r_e(Fe−C)	r_e(C−O)[a]
$FeCO^-$ $^4\Sigma^-$ $C_{\infty v}$	1.801 (1.860)	1.177 (1.194)
$Fe(CO)_2^-$ $^2\Pi_u$ $D_{\infty h}$	1.815	1.180
$Fe(CO)_2^-$ $^4\Pi_u$ $D_{\infty h}$	1.805	1.176
$Fe(CO)_3^-$ $^2A_1'$ D_{3h}	1.797	1.175
$Fe(CO)_4^-$ [b] $^2A_1$ C_{3v}		
axial	1.794	1.165
equatorial	1.799	1.167

[a] For comparison the bond length of free CO is 1.130 and 1.143 Å at the B3LYP and CCSD(T) levels of theory, respectively. [b] The $C_{ax}FeC_{eq}$ angle is 99.9° and the Fe−C−O angles are 180°. [c] The CCSD(T) parameters are given in parentheses. The bond lengths are in Å.

TABLE 3: Harmonic Frequencies Computed Using B3LYP, in cm^{-1}

		CO			
C−O	2211				
		$FeCO^-$			
bend(π)	208	Fe−C	437	C−O	1864
		$Fe(CO)_2^-$ $^4\Pi_u$ [a]			
bend(π_u)	73	bend(π'_u)	91	wag(π_g)	324
wag(π'_g)	393	wag(π_u)	432	Fe−C(σ_g)	444
Fe−C(σ_u)	452	wag(π'_u)	455	C−O(σ_u)	1866
C−O(σ_g)	1919				
		$Fe(CO)_2^-$ $^2\Pi_u$ [a]			
bend(π_u)	53	bend(π_u')	60	wag(π_g)	323
wag(π_g')	385	wag(π_u)	402	Fe−C(σ_g)	433
wag(π_u')	436	Fe−C(σ_u)	466	C−O(σ_g)	1860
C−O(σ_u)	1900				
		$Fe(CO)_3^-$			
bend(e′)	56	bend(a_2'')	71	wag(e″)	285
wag(a_2')	366	Fe−C(a_1')	434	Fe−C(e′)	506
wag(a_2'')	558	wag(e′)	583	C−O(e′)	1875
C−O(a_1')	1978				
		$Fe(CO)_4^-$ [b]			
bend(e)	62	bend(e)	80	bend(a_1)	86
wag(e)	341	wag(a_2)	365	Fe−C(a_1)	421
Fe−C(e)	472	Fe−C(a_1)	492	wag(e)	505
wag(a_1)	587	wag(e)	591	C−O(e)	1925
C−O(a_1)	1940	C−O(a_1)	2026		

[a] The calculations are performed as Π_{ux} or Π_{uy}, hence the degenerate modes are split and we list both components; the second component is denoted with a prime. [b] The Fe−C stretches and CO wags at 505, 587, and 591 cm^{-1} are somewhat mixed in character.

and the Fe−CO repulsion is reduced by sdσ and sp hybridization. Clearly, this mechanism cannot occur for $Fe(CO)_2^-$; if $Fe(CO)_2^-$ is linear, sp hybridization is lost, while if it is bent, as has been found in other ML_2 cases, sdσ hybridization is lost. Thus, in $Fe(CO)_2^-$ one of these σ electrons is transferred to the CO $2\pi^*$ orbital. We should note that this can also be viewed as a two-step process, where the Fe^- is promoted to a $3d^74s^1$-$4p^1$ occupation and the 4p electron is donated to the CO $2\pi^*$ orbitals.

The ground state of $Fe(CO)_3^-$ is $^2A'_1$ with D_{3h} symmetry. The bonding is perhaps easiest to view as being derived from a $3d^9$ occupation of Fe^-. Assume that the Fe atom and CO molecules are in the xy plane, with the Fe atom at the origin and one of the CO molecules along the y axis. To maximize the metal to CO $2\pi^*$ donation, the $3d_{xz}$ and $3d_{yz}$ orbitals are doubly occupied. The $3d_{xy}$ and $3d_{x^2-y^2}$ orbitals hybridize with the Fe $4p_x$ and $4p_y$ orbitals, respectively, to maximize the metal to CO $2\pi^*$ donation with the CO along the y axis and to minimize the repulsion with two 5σ orbitals of the other two CO molecules. This effect is clearly illustrated in a plot of the $4p\pi-3d\pi$ hybrid orbital—see Figure 1. The $3d_{2z^2-x^2-y^2}$ orbital has the same symmetry as the symmetric combination of the CO 5σ orbitals and is singly occupied to minimize the Fe−CO repulsion. We should note that because of the pd hybridization, the bonding in this molecule can also be viewed as being derived from the $3d^84p^1$ or $3d^74p^2$ occupations. As is clear from this analysis of the bonding, the D_{3h} structure is very favorable as it minimizes the ligand−ligand repulsion, and the polarization of the 3d orbitals that maximizes the donation to the CO $2\pi^*$ orbital also reduces the Fe−CO repulsion.

The lowest state of $Fe(CO)_4^-$ is $^2A_1$ and it has a C_{3v} symmetry. This system is derived from $Fe(CO)_3^-$ by adding an axial CO molecule along the z axis. The three equatorial CO molecules that are in the xy plane in $Fe(CO)_3^-$ bend out of the plane by 10°. The small bend retains the very favorable bonding described for $Fe(CO)_3^-$. The major difference in the bonding between $Fe(CO)_3^-$ and $Fe(CO)_4^-$ is the singly occupied orbital. To reduce the repulsion with the axial CO, the $3d_{2z^2-x^2-y^2}$ hybridizes with the Fe $4p_z$ orbital. The unpaired electron is located opposite to the axial CO and between the three equatorial CO molecules.

On the basis of their experiments, Villalta and Leopold[9] predicted the equilibrium bond lengths of the $X^3\Sigma^-$ and $a^5\Sigma^-$ states of FeCO relative to those in $FeCO^-$. In the analysis of the experimental data, one must make an assumption about relative change in the Fe−C and C−O bond lengths when the electron is detached. They performed the analysis making two assumptions, that both bond lengths could change in the same direction or in the opposite directions, but concluded that changes in the opposite direction were most likely. Our calculations show that the changes in the C−O and Fe−C bond lengths relative to $FeCO^-$ do occur in opposite direction for the $^5\Sigma^-$ state; the C−O bond length decreases and the Fe−C bond length increases. However, for the $^3\Sigma^-$ state we find that both bond lengths contract. That is, the C−O length decreases because there is less Fe to CO $2\pi^*$ donation and the Fe−C distance decreases because the removal of the σ electron decreases the Fe−CO repulsion. On the basis of our calculations, we compare with experimental analysis that agree with the signs of our computed changes in bond length. The B3LYP Fe−C bond length of 1.801 Å for $FeCO^-$ is between the B3LYP values of 1.770 and 1.912 Å [28] for the $^3\Sigma^-$ and $^5\Sigma^-$ states of FeCO, respectively, but closer to the $^3\Sigma^-$ state. The experimental differences for the $^3\Sigma^-$ and $^5\Sigma^-$ states are -0.05 ± 0.02 and $+0.07 \pm 0.02$ Å, respectively, which are in reasonable agreement with the computed values. The experimental CO contraction, relative to $FeCO^-$, is 0.03 ± 0.01 Å for both states, which is in good agreement with the B3LYP contractions of 0.028 and 0.023 Å for the $^3\Sigma^-$ and $^5\Sigma^-$ states, respectively. The CCSD(T) results for $FeCO^-$ and for the $^3\Sigma^-$ and $^5\Sigma^-$ states of FeCO[28,29] are consistent with those obtained using the B3LYP approach. Castro, Salahub, and Fournier[11] also report similar trends for the Fe−C and the C−O bond lengths using the LCGTO-DF approach. The B3LYP Fe−C stretching and the bending harmonic frequencies are in good agreement with experiment. The C−O stretching frequency of $FeCO^-$ has not been measured. Castro, Salahub, and Fournier predict a C−O frequency of 1831 cm^{-1} which is close to our B3LYP value of 1864 cm^{-1}. Thus, excluding the binding energy, the results of Castro, Salahub, and Fournier agree with those obtained in this work.

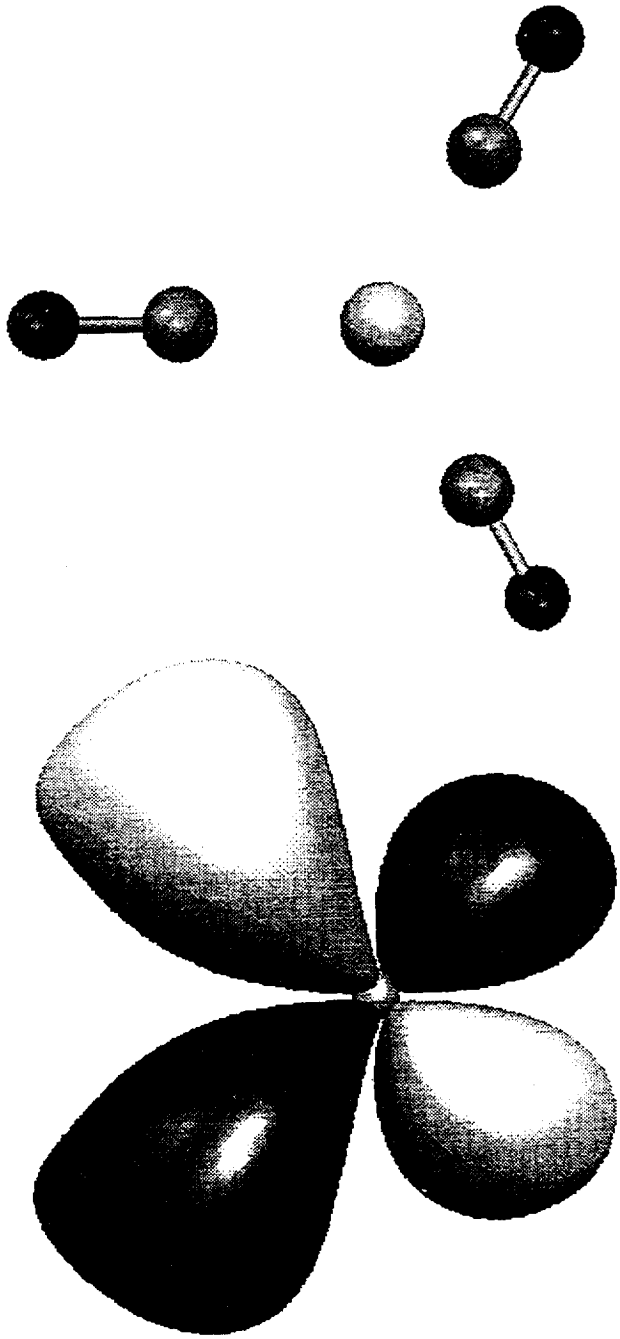

Figure 1. Isosurface of the pd hybrid orbital at cut-off values of ±0.12 au. The $Fe(CO)_3^-$ molecule is in the plane of the paper.

We now consider the trends in the CO binding energies. We first note that bonding in the positive ion is determined mostly by minimizing the Fe−CO repulsion, which is very different from the neutral or negative ion, where Fe donation to the CO $2\pi^*$ orbital is the most important factor in describing the bonding. Therefore, the difference in the trends in the CO binding energies for $Fe(CO)_n^-$ and $Fe(CO)_n^+$ is not too surprising and is easy to explain based on this work and that presented previously.[2] The present calculations explain the difference between the negative ion and neutral, as well as the trend on the negative ions. To aid in the discussion, we note that the CO binding energies (at 298 K) for the neutral systems are[3] 42.9 ± 3.5, 36.7 ± 3.5, 29.1 ± 5.8, and 27.9 ± 8.8 kcal/mol, where the first CO binding energy is given with respect to Fe $^3F(3d^74s^1)$, as this asymptote is to which it dissociates and is the most consistent with the dissociation for $FeCO^-$. Based on the corrections that we computed for $Fe(CO)_n^-$, these $Fe(CO)_n$ values would probably be reduced by 0.4−0.8 kcal/mol if corrected to 0 K.

The computed $Fe(CO)_n^-$ D_0 values are compared with experiment[3] in Table 1. The trend in the computed D_0 values agrees with experiment. Namely, the CO binding energies increase until the third, and then there is a small decrease for the fourth. This trend and the differences between the negative ion and neutral can be understood in terms of the bonding described above. For $FeCO^-$, the extra electron results in more Fe to $2\pi^*$ donation, which enhances the bonding relative to that in FeCO; however, the extra electron increases the σ repulsion. The sdσ and sp polarizations are efficient at reducing the repulsion for both the ion and neutral, but the extra σ repulsion results in the negative ion being about 10 kcal/mol less strongly bound. In $Fe(CO)_2^-$ the promotion of the electron from the 4s to the 4p orbital enhances the bonding, by reducing the σ repulsion and increasing the donation to the $2\pi^*$ orbital, but the binding energy is naturally reduced by the cost of this promotion. The similar first and second binding energies for $Fe(CO)_n^-$ indicate that the promotion energy is very similar in magnitude to the enhanced binding. However, the binding energy of $Fe(CO)_2^-$ is smaller than that in $Fe(CO)_2$ because $Fe(CO)_2$ does not have to pay the s to p promotion energy. For $Fe(CO)_3^-$ the promotion energy is now shared by three ligands and the binding energy is larger than in $Fe(CO)_2^-$. The binding energy in $Fe(CO)_3^-$ is significantly larger than that in $Fe(CO)_3$ because the extra electron in the negative ion allows for a much larger donation to the $2\pi^*$ orbitals. The binding energy of $Fe(CO)_4^-$ is slightly smaller than that of $Fe(CO)_3^-$. This is not too surprising given the very similar binding in these two systems. The extra CO results in a larger ligand−ligand repulsion and slightly smaller $2\pi^*$ donation per CO. This results in a decrease in the binding energy even though the promotion energy is now shared by four CO molecules. The extra electron again results in the negative ion being significantly more strongly bound than the neutral.

In addition to the trend in the computed D_0 values being consistent with experiment, the computed B3LYP values for $Fe(CO)_2^-$, $Fe(CO)_3^-$, and $Fe(CO)_4^-$ agree well with experiment; the computed values for $Fe(CO)_2^-$ and $Fe(CO)_4^-$ fall within the experimental error bars and $Fe(CO)_3^-$ is only 0.3 kcal/mol larger than the experimental upper bound. Unlike these values, the computed B3LYP result for $FeCO^-$ is significantly smaller than the experimental result. The results obtained using the CCSD(T) approach are larger than the B3LYP result but are still much smaller than that from experiment. It is very difficult to assign all of this difference to an error in experiment because the CCSD(T) result[29] for FeCO is about 2 kcal/mol smaller than the most accurate experimental value,[9] which is derived from the experimental $FeCO^-$ D_{298} value. Both the B3LYP and CCSD(T) agree[28] with experiment for $FeCO^+$, while the B3LYP result[28] is too small for FeCO and the CCSD(T) agrees[29] with experiment, and both are too small for $FeCO^-$. This suggests that as the Fe to $2\pi^*$ donation increases, the system becomes harder to describe using a single reference-based approach. We should also note that we have found that the error in the B3LYP approach is often the largest for the first binding energy and that part of this error arises from a description of the metal atom. In Table 4 we compare the computed and experimental[30] electron affinity (EA) of Fe. The B3LYP value is significantly too large because the B3LYP is biased in favor of metal occupations with a larger number of 3d electrons. The Fe population in $FeCO^-$ is between Fe and Fe^-, and the 3d populations is between six and seven. Thus, a second method of computing the binding energy would be to dissociate to CO + Fe $^5D(3d^64s^2)$ + e^- and correct this to the CO + Fe^- $^4F(3d^74s^2)$ asymptote using the experimental EA. This results in an $FeCO^-$ B3LYP binding energy of 37.0 kcal/mol. This argument is too simplistic, however, as applying this approach would make the CCSD(T) result in worse agreement with experiment. Thus, while this error in the description of Fe^- is probably the origin of part of the error in the B3LYP approach, it cannot be used to compute a more accurate value. Despite the small D_0 value for $FeCO^-$, the experiments of Villalta and Leopold[9] confirm that we have correctly described the nature of the bonding in $FeCO^-$ and thus that our analyses of the bonding and trends are correct.

TABLE 4: Comparison of the Computed Fe Electron Affinity (kcal/mol) with Experiment

	B3LYP	CCSD(T)	expt[a]
Fe^- $^4F(3d^74s^2)$−Fe $^5D(3d^64s^2)$	14.5	−7.8	3.5 ± 0.1
error	10.7	−11.6	

[a] Reference 30.

IV. Conclusions

The computed changes in geometry between $FeCO^-$ and the $X^3\Sigma^-$ and $a^5\Sigma^-$ states of FeCO are in reasonable agreement with experiment, as are the computed $FeCO^-$ frequencies. However, the computed Fe^-−CO binding energy is too small. The second, third, and fourth CO binding energies are in good agreement with experiment. For $FeCO^-$ the calculations show that sdσ and sp hybridizations reduce the Fe−CO repulsion. With the addition of the second CO molecule, there is a promotion of one of these Fe σ valence electrons to the CO $2\pi^*$ orbital. This reduces the σ repulsion and increases the π bonding. However, the first and second CO binding energies are very similar because of the cost of this promotion. In $Fe(CO)_3^-$ and $Fe(CO)_4^-$ the cost of this promotion is shared by more ligands, resulting in third and fourth CO binding energies that are significantly larger than the first two. The bonding in $Fe(CO)_3^-$ and $Fe(CO)_4^-$ is very similar and the smaller $2\pi^*$ donation per CO and the larger ligand−ligand repulsion results in a slightly smaller binding energy for the fourth CO than for the third. The calculations also explain the difference in the trends in the binding energies for the neutral and negative ion.

Acknowledgment. The authors acknowledge many helpful discussions with Doreen Leopold. A.R. acknowledges an NRC fellowship.

References and Notes

(1) Bauschlicher, C. W.; Langhoff, S. R.; Partridge, H. *J. Chem. Phys.* **1991**, *94*, 2068.

(2) Ricca, A.; Bauschlicher, C. W. *J. Phys. Chem.* **1994**, *98*, 12899.
(3) Sunderlin, L. S.; Wang, D.; Squires, R. R. *J. Am. Chem. Soc.* **1992**, *114*, 2788.
(4) Distefano, G. *J. Res. Nat. Bur. Stand., Sect. A* **1970**, *74*, 233, as corrected by Halle, L. F.; Armentrout, P. B.; Beauchamp, J. L. *Organometallics* **1982**, *1*, 963.
(5) Norwood, K.; Ali, A.; Flesch, G. D.; Ng, C. Y. *J. Am. Chem. Soc.* **1990**, *112*, 7502.
(6) Schultz, R. H.; Crellin, K. C.; Armentrout, P. B. *J. Am. Chem. Soc.* **1991**, *113*, 8590.
(7) Dalleska, N. F.; Honma, K., Sunderlin, L. S.; Armentrout, P. B. *J. Am. Chem. Soc.* **1994**, *116*, 3519.
(8) Schultz, R. H.; Armentrout, P. B. *J. Phys. Chem.* **1993**, *97*, 596.
(9) Villalta, P. W.; Leopold, D. G. *J. Chem. Phys.* **1993**, *98*, 7730.
(10) Engelking, P. C.; Lineberger, W. C. *J. Am. Chem. Soc.* **1979**, *101*, 5569.
(11) Castro, M.; Salahub, D. R.; Fournier, R. *J. Chem. Phys.* **1994**, *100*, 8233.
(12) Wachters, A. J. H. *J. Chem. Phys.* **1970**, *52*, 1033.
(13) Hay, P. J. *J. Chem. Phys.* **1977**, *66*, 4377.
(14) Huzinaga, S. *J. Chem. Phys.* **1965**, *42*, 1293.
(15) Dunning, T. H. *J. Chem. Phys.* **1989**, *90*, 1007. Kendall, R. A.; Dunning, T. H.; Harrison, R. J. *J. Chem. Phys.* **1992**, *96*, 6796.
(16) Bauschlicher, C. W.; Taylor, P. R. *Theor. Chim. Acta* **1993**, *86*, 13 and tabulated in Bauschlicher, C. W. *Theor. Chim. Acta*, in press.
(17) Stevens, P. J.; Devlin, F. J.; Chablowski, C. F.; Frisch, M. J. *J. Phys. Chem.* **1994**, *98*, 11623.
(18) Becke, A. D. *J. Chem. Phys.* **1993**, *98*, 5648.
(19) Becke, A. D. *Phys. Rev. A.* **1988**, *38*, 3098.
(20) Lee, C.; Yang, W.; Parr, R. G. *Phys. Rev. B* **1988**, *37*, 785.
(21) Vosko, S. H.; Wilk, L.; Nusair, M. *Can. J. Phys.* **1980**, *58*, 1200.
(22) Bartlett, R. J. *Annu. Rev. Phys. Chem.* **1981**, *32*, 359.
(23) Raghavachari, K.; Trucks, G. W.; Pople, J. A.; Head-Gordon, M. *Chem. Phys. Lett.* **1989**, *157*, 479.
(24) Knowles, P. J.; Hampel, C.; Werner, H.-J. *J. Chem. Phys.* **1993**, *99*, 5219.
(25) Frisch, M. J.; Trucks, G. .W; Schlegel, H. B.; Gill, P. M. W.; Johnson, B. G.; Wong, M. W.; Foresman, J. B.; Robb, M. A.; Head-Gordon, M.; Replogle, E. S.; Gomperts, R.; Andres, J. L.; Raghavachari, K.; Binkley, J. S.; Gonzalez, C.; Martin, R. L.; Fox, D. J.; Defrees, J.; Baker, J.; Stewart, J. J. P.; Pople, J. A. *Gaussian 92/DFT*, Revision G.2; Gaussian, Inc.: Pittsburgh, PA, 1993.
(26) MOLPRO 94 is a package of *ab initio* programs written by H.-J. Werner and P. J. Knowles, with contributions from J. Almlöf, R. D. Amos, M. J. O. Deegan, S. T. Elbert, C. Hampel, W. Meyer, K. Peterson, R. Pitzer, A. J. Stone, and P. R. Taylor.
(27) Flükiger, P. F. Development of the Molecular Graphics Package MOLEKEL and its Application to Selected Problems in Organic and Organometallic Chemistry. Ph.D. Thesis 2561, University of Geneva, 1992.
(28) Ricca, A.; Bauschlicher, C. W. *Theor. Chim. Acta*, in press.
(29) Ricca, A.; Bauschlicher, C. W.; Rosi, M. *J. Phys. Chem.* **1994**, *98*, 9498.
(30) Leopold, D. G.; Lineberger, W. C. *J. Chem. Phys.* **1986**, *85*, 51.

JP9428799